JOURNAL OF MATERIALS SCIENCE 5 (1970) 394–406

Order-Induced Strengthening in Ni_4Mo

B. CHAKRAVARTI, E. A. STARKE JR, B. G. LEFEVRE
Metallurgy Program, School of Chemical Engineering, Georgia Institute of Technology, Atlanta, Georgia, USA

Polycrystalline samples of Ni_4Mo have been examined at various stages of isothermal ageing at 700° C. The mechanical properties were measured on initially disordered samples at various stages of the ordering process. These properties were correlated with microstructural observations such as domain size, degree of order and fracture characteristics. The correlations are rationalised in terms of a model for the ordering process and its effect on dislocation motion.

1. Introduction

It is well known that the deformation behaviour of crystals is highly structure-sensitive, being influenced by a variety of defects which may be present before, or formed during, the deformation process. If a crystal contains more than one atomic species, a further influence on the mechanical behaviour is exhibited by local atomic arrangements. Four general types of arrangement are possible on a particular lattice in a solid solution: (a) random, in which there is no preference by an atom for a type of neighbour or particular lattice site [1, 2], (b) short-range order, in which a given atomic species exhibits a statistical preference for unlike neighbours but not for a particular lattice site [1, 3], (c) clustering, in which a given atomic species exhibits a statistical preference for like neighbours but not for a particular lattice site [4], and (d) long-range order, in which the different atomic species occupies preferred sites on the crystal lattice [5, 6]. The references cited for each arrangement refer to reviews of theories on strengthening mechanisms attributed to these various arrangements.

The present paper is concerned with order-strengthening induced when a previously disordered alloy undergoes a transition to long-range order. The transition from random or short-range order to long-range order usually occurs at some critical temperature during cooling. The completeness of the transition or the degree of long-range order may be varied by certain thermal and/or mechanical treatments and is usually described by the LRO parameter S. Warren [7] has defined this parameter as

$$S = (r_A - X_A)/Y_B = (r_B - X_B)/Y_A,$$

where r_A and r_B are respectively the fraction of A-sites and of B-sites occupied by the correct atoms, X_A and X_B are the atomic fractions of A and B atoms, and Y_A and Y_B are the fractions of A and B lattice sites. For a stoichiometric alloy S is, therefore, zero when the alloy is perfectly random, and one when perfectly ordered.

Depending on the particular alloy system, the disorder-to-order transformation may occur either homogeneously or heterogeneously [8]. In addition, the crystal system may or may not be altered. Cu_3Au, for example, has a cubic structure both in the ordered and disordered states. In contrast, Ni_4Mo changes from cubic in the disordered condition (α-phase) to tetragonal in the ordered state (β-phase), having a contraction of 0.5% in a_0 and 1.0% in c_0 of the cubic lattice [9].

Alloys which undergo a distortion or crystal structure change during the transition offer the greatest potential in order-strengthening; however, there have been only a few studies on alloys of this type, mainly on CuAu [10-12]. Ni-Mo alloys have been found to respond readily to age-hardening treatments in the β-region after quenching from above the transformation temperature [13-15]. Although the agreement of the data is not particularly good, the investigators all agree that large hardness increases can be produced within a few tenths of an hour by annealing in the temperature range of 600 to 800° C. The time-temperature transformation curve for the ordering process of Ni_4Mo has a

"C" shape with the nose of the curve around 710 to 775° C [16, 17]. The kinetics and morphology of the ordering process in this alloy has recently received attention [16-23].

The present study was undertaken in an effort to understand order-hardening in alloys which undergo a crystal structure change during ordering. Ni_4Mo was chosen for the study since previous experience showed this alloy to be conducive to microscopic studies by X-ray diffraction, electron and field ion microscopy techniques. We felt that structural modifications which accompany the disorder-order transitions and which could be correlated with mechanical property measurements would help elucidate order-strengthening in Ni_4Mo alloys.

2. Experimental

Alloys were prepared by arc-melting in an argon atmosphere from high purity nickel and molybdenum to form Ni_4Mo. Each sample was melted six times to ensure adequate mixing of the nickel and molybdenum. The as-cast ingots were cold-rolled to a 50% reduction in thickness to break up the cast structure, homogenised in vacuum at 1000° C for one week and quenched in iced brine. They were then rolled to a thickness of 0.38 cm and machined to a thickness of 0.32 cm.

The compositions of the samples were determined from lattice parameter measurements made on stress-relieved −325 mesh filings using high purity aluminium as an internal standard. The data of Guthrie and Stansbury [13] were used for calculating the composition from the lattice parameter measurements. The molybdenum contents of the samples used in this study are given in table I.

Tensile samples were machined according to ASTM E8-66 for sub-size specimens. The stresses induced by the machining operation were removed during a final disordering heat-treatment of 5 h at 1000° C followed by iced brine quenching.

The ordering temperature and times to be used for extensive study were determined by preliminary investigations using hardness measurements. Samples 1 cm square were ordered in vacuum for various times at 700, 750, 800 and 850° C. The hardness was measured using a Tukon Tester and a 500 g load. The critical ordering temperature, T_c, has been given as 868° C [13]. The results of these measurements are given in fig. 1. There was no response to the 850° C heat-treatment after 4 h, so treatments at this temperature were discontinued. The hardening rate at both 750 and 800° C were adequate; however, the ordering process induced cracks in the samples. The times and the temperatures at which cracking was observed are denoted by asterisks in fig. 1. No cracking was ever observed on samples treated at 700° C although a marked increase in hardness was observed after short times at this temperature. Consequently, 700° C was chosen for the ordering treatments for structural/mechanical property correlations.

The degree of order after various heat-treatments was determined by X-ray techniques using monochromated CuKα radiation and a modified GE XRD-6 diffractometer described elsewhere [24]. The preferred orientation of the samples combined with the superposition of fundamental and superlattice reflections of polycrystalline Ni_4Mo necessitated the usage of the technique devised by LeFevre and Starke [25] for order parameter determination. The order parameter was measured on each tensile sample prior to testing. The average domain size was also determined by X-ray diffraction using Scherrer's equation. The $(1\,1\,0)_T$* superlattice peak was used for these calculations and was corrected for strain and instrumental broadening by comparison with the nearby $(2\,1\,1)_T$ fundamental peak.

The tensile tests were conducted on an Instron testing machine using a one-inch extensometer and a strain rate of 0.05 per minute. Three samples (A0, C100, E15H) were pulled to fracture and two others to about 5% plastic strain. The fracture surfaces were examined by scanning electron microscopy using a Cambridge Stereoscan Mark II. Slices were spark-cut from each of the tensile samples, ground to 0.025 cm and small discs punched out for observation in the

TABLE I

Alloy no.	Weight %	Atomic %	Alloy no.	Weight %	Atomic %
A0	27.30	18.69	D180	27.80	19.07
B40	27.85	19.10	E15H	27.40	18.76
C100	27.55	18.88			

* Subscript T refers to the tetragonal indices and subscript C refers to the cubic.

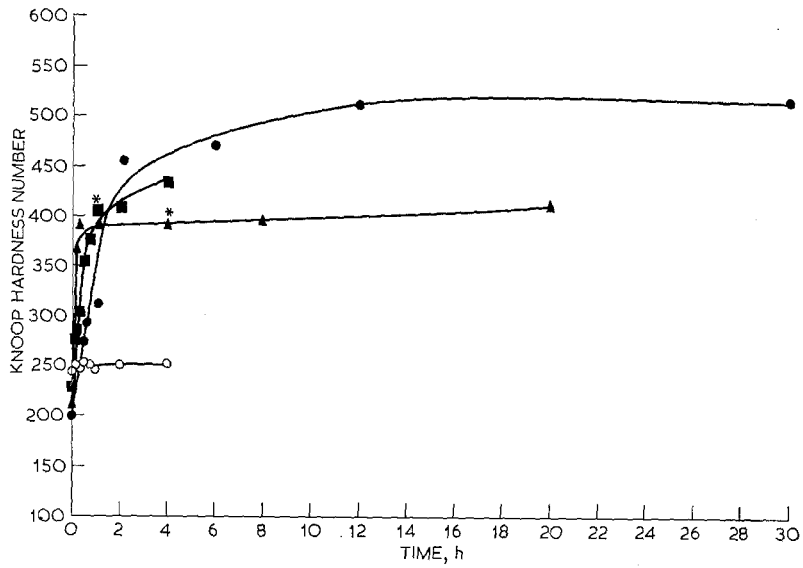

Figure 1 Microhardness of Ni_4Mo at 25° C measured as a function of ageing time at various temperatures after quenching from 1000° C. ○—○ 850° C; ■—■ 800° C; ▲—▲ 750° C; ●—● 700° C.

electron microscope. The discs were jet-polished at 0° C using a solution of two parts sulphuric acid and one part water. Electron microscopic observations were made in transmission in both a Siemens 1A and a JEM 7A microscope at 100 kV. Samples for field-ion studies were cut from similar slices used for electron microscopy. The field-ion samples were electropolished in the sulphuric acid solution to fine wire form and imaged in helium at liquid hydrogen temperature.

3. Experimental Results

The ordering sequence of Ni_4Mo has been

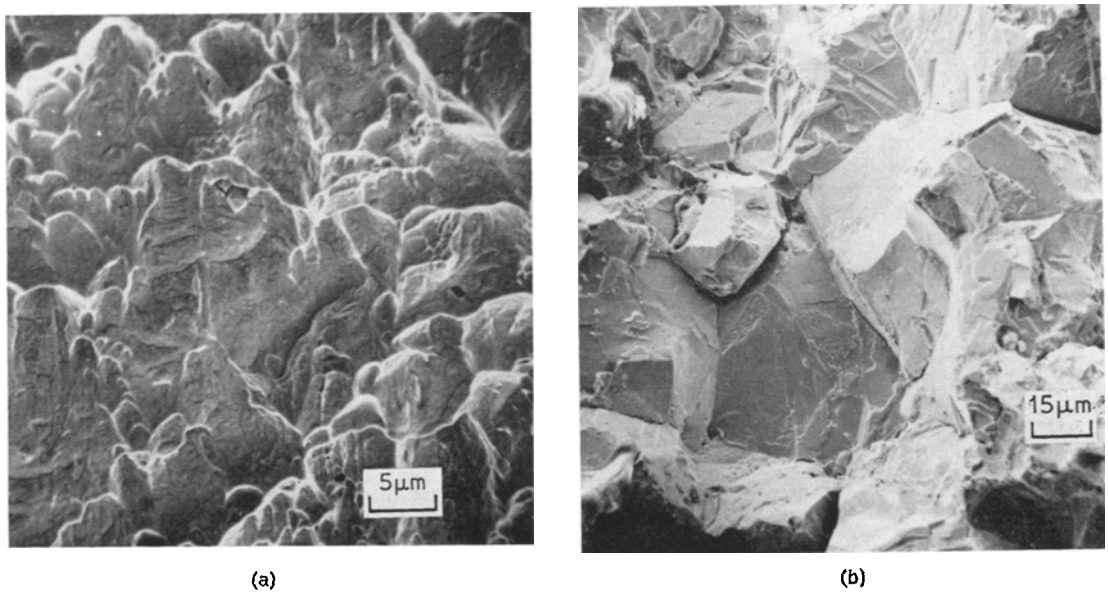

(a) (b)

Figure 2 Scanning electron micrographs of the fracture surfaces of Ni_4Mo in (a) the disordered condition and (b) after ageing for 15 h at 700° C with $S = 1$.

TABLE II

Alloy no.	Ageing time	Degree of order, S	Domain size (Å)	Yield stress (kg cm^{-2})	% elongation	% reduction in area	Work hardening coefficient $\times 10^2$
A0	quenched	0.0	—	3500	60.0	43.0	33.7
B40	40 min	0.64	46	6200	—	—	—
C100	100 min	0.76	54	6720	26.0	22.4	36.8
D180	180 min	0.81	74	7340	—	—	—
E15H	15 h	1.00	106	7635	3.2	3.15	52

followed at 700° C by structural and mechanical studies. Tensile tests provided strength and fracture data of the alloy at various stages of the ageing process. X-ray diffraction techniques were employed along with electron and field-ion microscopy to obtain detailed information on the nature of the structure responsible for the mechanical properties, and to elucidate the ordering mechanism.

Table II gives the results of the tensile tests after various ageing times along with the corresponding degree of order and antiphase domain size as determined from X-ray measurements. The yield stress rises sharply initially but levels off after an ageing treatment of 100 min. The total increases in strength of 4100 kg cm^{-2} and work-hardening coefficient of 18.3 $\times$ 10^2 after 15 h ageing were accompanied by a change in the LRO parameter from zero to one, and an increase in the antiphase domain size to 106 Å. In addition, the elongation decreased from 60% in the disordered sample to 3.2% in the fully ordered sample and was accompanied by a change in fracture mode from transgranular, fig. 2a, to intergranular, fig. 2b.

The electron microscopy studies showed that the disordered alloy exhibited large equiaxed grains, $\sim$ 40 μm, and numerous annealing twins, indicating a completely recrystallised structure. Considerable short-range order was present, as evidenced by the appearance of diffuse spots in the electron diffraction pattern [18, 19, 23], and numerous paired dislocations [26-30] in the micrographs. A very fine "mottle" contrast was visible in the vicinity of the bend extinction contours similar to that observed by Ruedl *et al* [19] and Snyder and Brooks [23]. Dark field images obtained by placing the objective aperture over a diffuse spot failed to show any distinct microdomains in the short-range-ordered structure.

The ordering transformation of Ni_4Mo at 700° C was revealed, by the electron microscopy studies, to occur by two distinct mechanisms. The early stage was characterised by the development of a fine cross-textured contrast appearing uniformly within the grains. A representation of this stage, which will be referred to as the *homogeneous component*, is presented in fig. 3a which characterises a sample aged for 40 min at 700° C. The contrast was produced by an operating fundamental reflection and the striations were shown by standard trace analysis methods to be approximately parallel to $\{1\,1\,2\}_C$ plane traces. Selected area diffraction patterns showed the presence of superlattice spots from all of the six possible domain orientations. However, the usual antiphase boundary contrast present in ordered alloys [31] was never observed even with extensive tilting of the specimen. This was assumed to be due to the fineness of the structure which was verified by field-ion microscopy studies to be discussed later. No distinct relrods were observed in the diffraction patterns as one might expect from small particle or strain effects (fig. 3b). Further annealing at 700° C for a total time of 100 min produced no significant changes in either the micrographs or the electron diffraction patterns except for a slight coarsening of the cross-textured contrast.

After 180 min a second ordering mechanism was initiated, as shown by the presence of a *heterogeneous component* which appeared at the α-grain boundaries (fig. 4). Such contrast effects have been observed in Ni_4Mo after ageing at 775° C [23] as well as in other ordering systems involving a cubic to tetragonal transition [10, 23, 32]. The contrast within the heterogeneous region is very similar to the appearance of the columnar grain structure in a metal casting with the long dimension perpendicular to the grain-boundary. Close inspection, fig. 4b, shows that along one edge it appears to be continuous with the homogeneous component of one grain while along the opposite edge it is separated from the continuous component of the adjacent grain by a sharp and apparently incoherent interface.

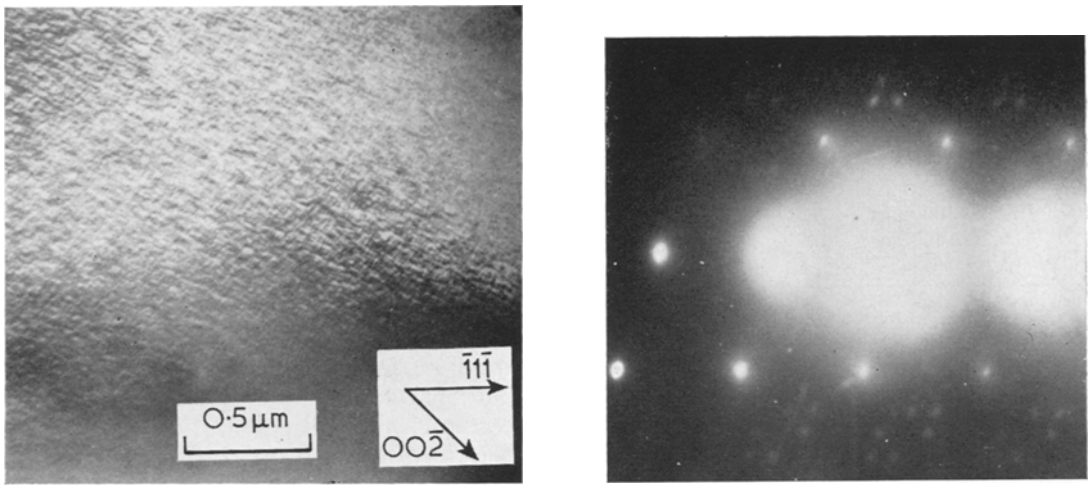

(a) (b)

Figure 3 (a) Transmission electron micrograph of Ni_4Mo after 40 min at 700° C showing fine cross-textured contrast within the grains. (b) A diffraction pattern from the cross-textured region showing superlattice spots from differently oriented domains.

Tanner [33] has described a similar reaction product in Ni_2V as a coherent allotriomorph which forms coherently with one grain and grows into the adjacent grain by migration of the incoherent grain-boundary. A similar effect in CuAu has been described by Arunachalam and Cahn [10] as recrystallisation by stress-induced boundary migration.

The heterogeneous component grew continuously with further ageing and after 15 h at 700° C it comprised approximately one-third of the total volume of the structure. Contrast effects from the various types of interfaces (antiparallel twin boundaries, perpendicular twin boundaries and antiphase boundaries) previously discussed by Ruedl, *et al* [19] were clearly distinguishable in this region (fig. 5a and b). The "perpendicular twins"* indicated by the δ-fringes of fig. 5a were found to be very thin platelets lying parallel to $\{110\}_C$ planes. By careful tilting of the foil it was determined that in most cases what appeared to be the boundary

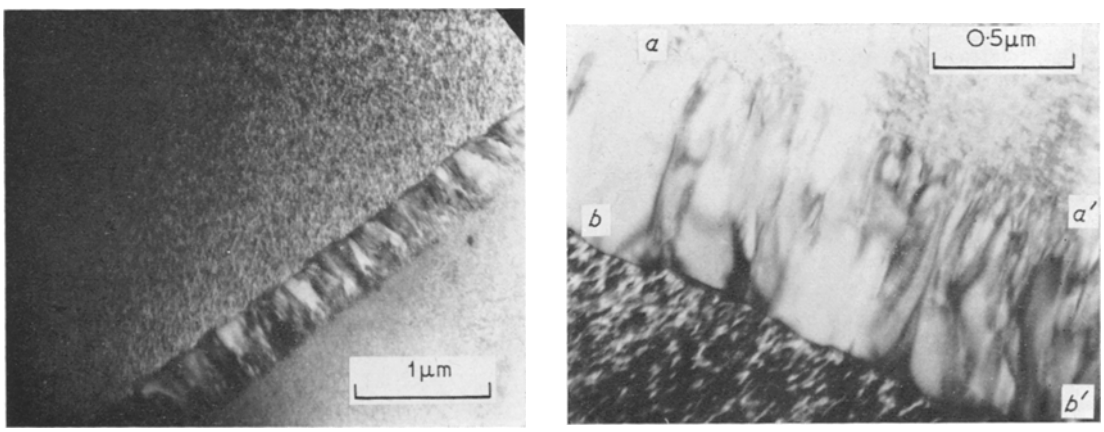

(a) (b)

Figure 4 (a) The heterogeneous component appearing in the α-grain boundaries after 180 min at 700° C. (b) Enlarged view of the heterogeneous component. It is continuous with the homogeneous component along *a–a′* but discontinuous along *b–b′*.

* i.e. twins in which the orientations of the tetragonal axes were approximately mutually perpendicular.

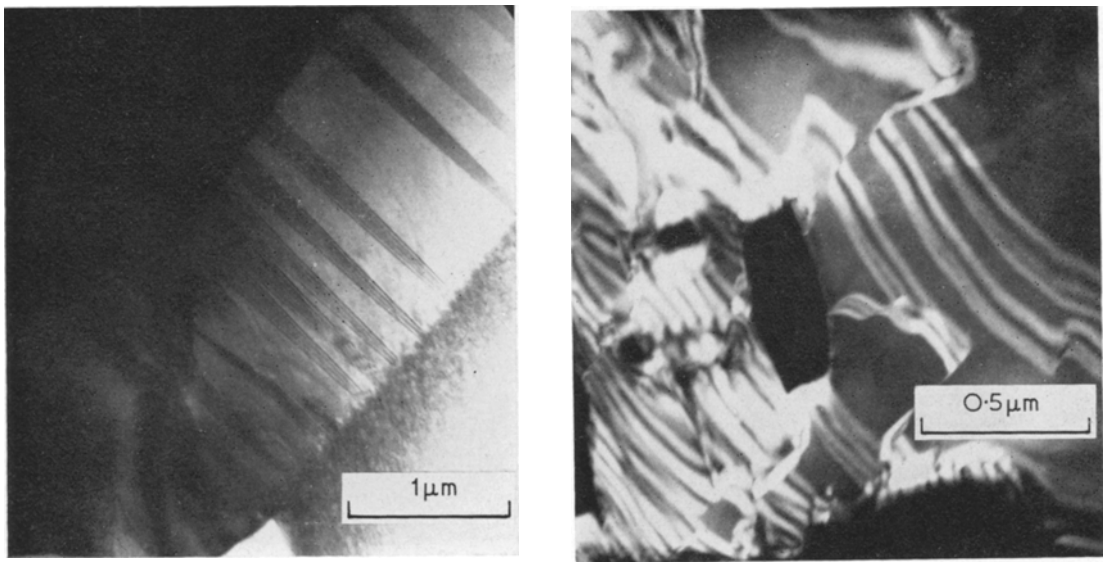

(a) (b)

Figure 5 Contrast features within the heterogeneous region after 15 h at 700° C: (a) δ-fringe contrast from perpendicular twins. (b) Dark field image with a superlattice reflection showing antiphase boundaries.

between adjacent twin related domains was, in fact, an entire twinned region, so thin its boundaries completely overlapped. This was further supported by field-ion microscopy studies.

The field-ion studies were undertaken to elucidate more precisely the nature of the microstructure of the alloy in the partially ordered state. From the available X-ray and electron microscopy data one cannot accurately determine the domain size and shape nor how the degree or order varies locally within a microstructure such as that exhibited in fig. 3a. For the purpose of this study it was important to know whether the fine cross-textured contrast was indicative of a structure which was truly homogeneous or heterogeneous, i.e. a two-phase mixture of ordered and disordered regions. The difficulty of differentiating contrast effects due to phase boundaries from those due to coherency strains in electron micrographs of a fine structure such as this has been stressed by Tanner [32, 34]. On the other hand it has been shown that field-ion images can be used to determine the domain structure and obtain a qualitative measure of the order parameter on an atomic scale [21, 22, 35-40].

Field-ion micrographs depicting the microstructure of the homogeneous component are presented in fig. 6. The treatment of the sample represented by fig. 6d was not a direct part of the present study and serves only as an aid in interpretation. The degree of order is represented in the micrographs by the local regularity of the image and the domain boundaries by discontinuities in the image symmetry [21]. It can be seen that the 40 min anneal produced a microstructure of uniformly ordered material consisting of many contiguous domains in which the order is less than perfect. No evidence was ever seen in such images of the co-existence of ordered and disordered regions* as one would expect in a classic nucleation and growth process. Hence this structure has the appearance one would expect from a homogeneous ordering process. The fact that the image is somewhat less regular than that of the fully ordered structure of fig. 6c is in qualitative agreement with the LRO parameter of 0.6 determined by X-ray measurements. This was further reflected by the lack of complete stability of the specimen during the imaging process. It is characteristic of this material that disordered specimens are in a dynamic state of irregular field evaporation during imaging whereas the completely ordered specimens are quite stable.

The average domain size of the 40 min anneal

* The regional darkness seen in these micrographs is not to be confused with heterogeneity in the structure. This occurs in the vicinity of low index poles of the cubic lattice and results from the effect of crystallographic anisotropy on the basic imaging process.

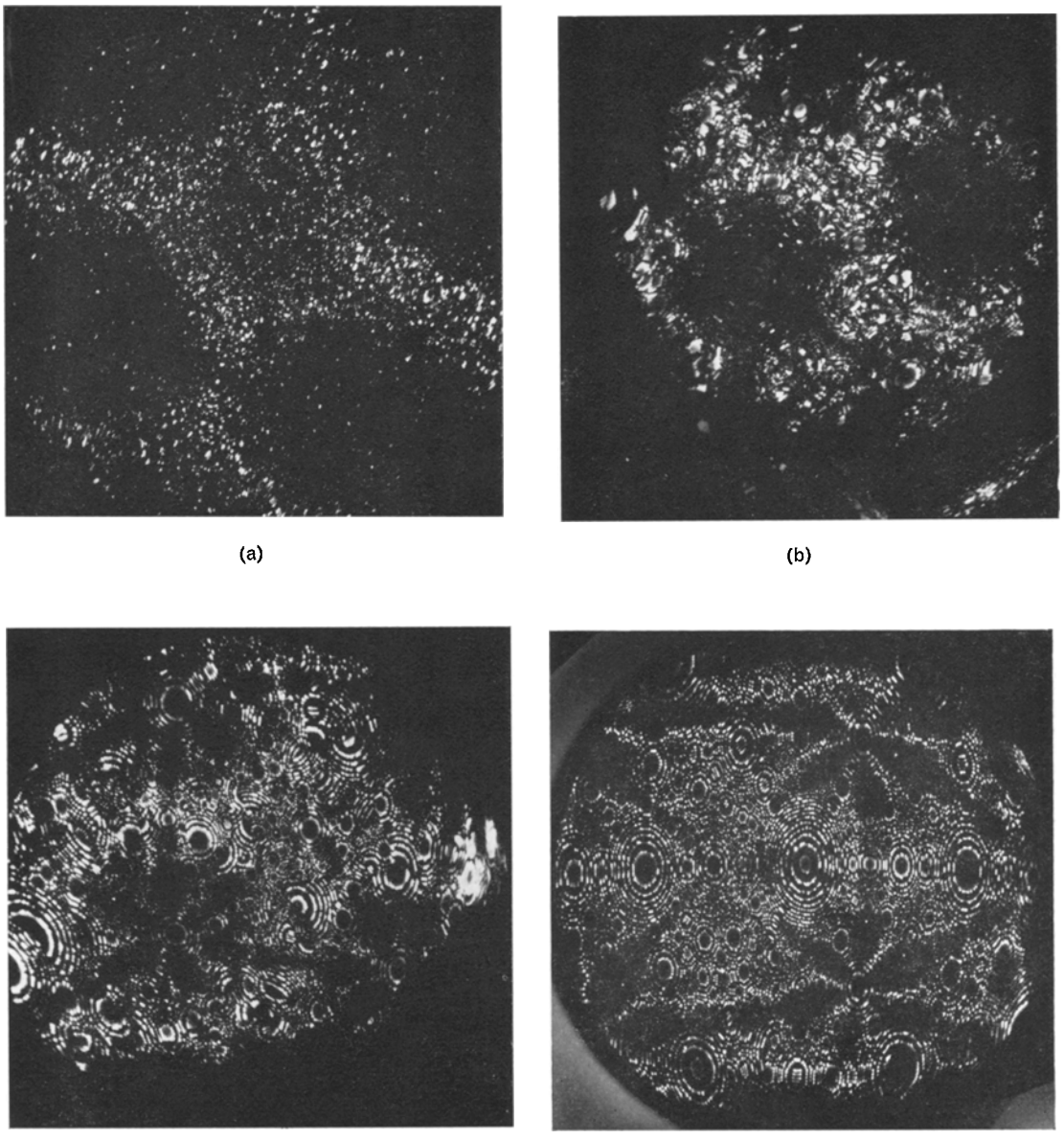

(a) (b)

(c) (d)

Figure 6 Field-ion micrographs of Ni_4Mo in various conditions: (a) disordered; (b) annealed 40 min at 700° C; (c) annealed 15 h at 700° C; (d) annealed 300 h at 750° C to produce fully-ordered large domains for comparison.

appears to be in the range of 20 to 50 Å* which is also in rough agreement with the domain size determined from the X-ray measurements. It is clear from this evidence why individual domains were not resolved in the electron microscope. The domain boundary network can be made to show more prominently by photographing the specimen during field evaporation, as shown in fig. 7. It can be seen that the domains show a tendency to be elongated in a direction indicated by the arrows. Within the accuracy of the analysis this direction was found to be parallel to a $\{1\,1\,2\}_C$ plane trace, in agreement with the orientation of the striations in the electron

* Field-ion micrographs approximate pseudo-sterographic projections. Since the linear magnification varies from centre to edge, micron markers would not be meaningful; however, a rough measure of the magnification can be obtained from the fact that the linear distance across the imaged region of each of the micrographs is approximately 1500 to 2000 Å.

micrographs. This observation is significant because there appears to be some question as to whether similar striae in other systems represent the true domain shape or simply the direction of attendant coherency strains. It would appear that in Ni_4Mo one is seeing the true domain shape in the fine striae of the electron micrographs. The changes in the structure of the homogeneous component with increasing ageing times can be seen by comparing fig. 6b with fig. 6c. The domains increase in size from the 20 to 50 Å, present after 40 min, to the 100 to 200 Å after 15 h, and the degree of order within the domains also increases. The results are in agreement with the electron microscopy and X-ray results.

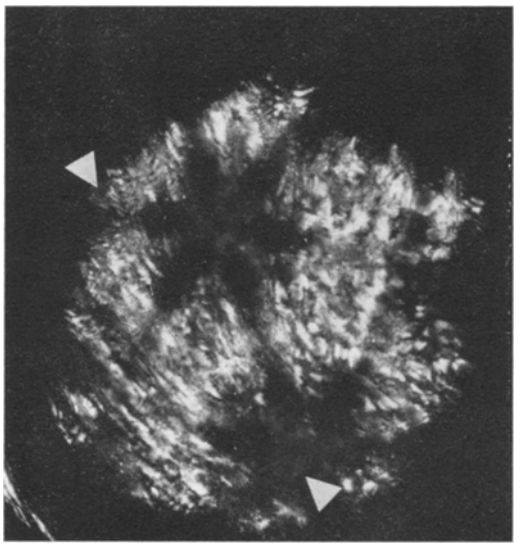

Figure 7 Field-ion micrograph of Ni_4Mo annealed for 40 min at 700° C and taken during field evaporation. The domains show a tendency to be elongated in a direction parallel to the arrows

Fig. 8 shows a specimen with an extremely high density of the thin plate-like perpendicular twins photographed during field evaporation to enhance the appearance of the boundaries. The anneal given (750° C for 20 h) was again not a direct part of the present study; however, it was known from prior experience that such a condition produces a high density of the twins so that the maximum probability of encountering them in the field-ion specimen would exist. It can be seen here that many of the twins are only a few atomic diameters thick, as had been concluded in the electron microscopy results discussed earlier.

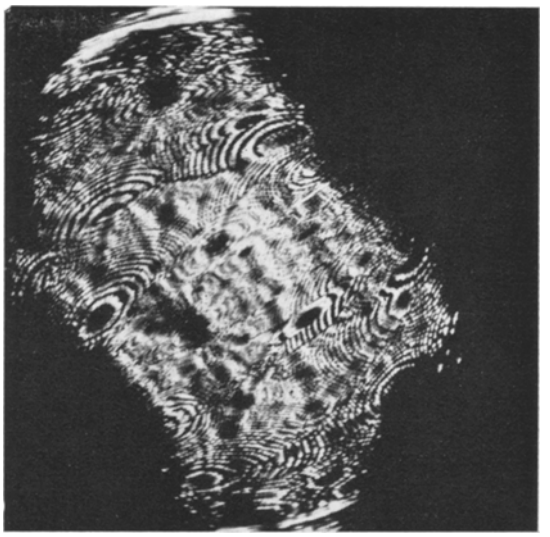

Figure 8 Field-ion micrograph of Ni_4Mo showing high density of perpendicular twins. Annealed at 750° C for 20 h.

4. Discussion

4.1. Ordering of Ni_4Mo

In the present paper the usual controversy which surrounds most discussions on order-disorder reactions, i.e. whether or not they should be considered as first or second order transformations, will not be discussed. It should not be necessary to prove that in a system such as Ni_4Mo, in which the ordered and disordered states differ in crystal structure, the ordering reaction could be anything but a classical phase change, i.e. a first order transformation [41]. Instead, the present discussion will concentrate on the mechanism by which the Ni_4Mo alloy proceeds from the disordered to the ordered state. Transformations cannot be classified as to first or second order on the basis of kinetic considerations since these can be greatly varied by seemingly insignificant changes in heat-treatment procedure.

The ordering of Ni_4Mo below the critical temperature T_c, has been considered to proceed by nucleation and growth of microdomains which exist above T_c. This concept was first presented by Spruiell [18] who suggested a model for short-range order above T_c similar to long-range ordered Ni_4Mo. Experimental support for this model has been presented by Ruedl *et al* [19]. In addition, Snyder and Brooks [23] have used this concept in discussing isothermal ordering of Ni_4Mo at 775° C. On the other hand, theoretical considerations of interaction

energies have led Clapp and Moss [42] to suggest that the microdomain theory might not be particularly useful in this system and that the short-range order could best be explained by the statistical theory.

There have been many discussions on other systems, which undergo a crystal structure change during ordering, as to whether the reaction occurs homogeneously or by nucleation and growth [43-48]. The presence of microdomains above T_c has implied to some workers [49] a nucleation and growth concept below T_c, whereas the statistical SRO model might imply homogeneous ordering below this temperature. The concept of microdomains above the critical temperature has actually been very hazily defined. These domains are normally considered to be of small size and vary in degree of order. As the size of the domains decreases the statistical model for short-range order is approached and the domains lose their individual identity [50]. Likewise the distinction between homogeneous ordering and a nucleation and growth process in Ni_4Mo during isothermal annealing below T_c becomes almost irrelevant and simply a matter of semantics as the annealing temperature is reduced. The volume free energy of ordering normally increases with decreasing temperature and for Ni_4Mo the interface coherency strain energy also decreases with decreasing temperature. The latter result may be inferred from dilatometry measurements of Stansbury [51]. The variation of these parameters with temperature indicates that as the ordering temperature is lowered, small nuclei become more stable and the frequency of nucleation is increased [48]. Consequently, at a "low ordering temperature" the frequency of nucleation is so high and the nuclei so small that the material is homogeneous; i.e. impingement between the domains is instantaneous and there is essentially no "two-phase" region between an ordered nucleus or microdomain and a disordered matrix. After impingement the mobility of the boundaries is reduced since there is no change in composition or structure across the interface. Ordering then proceeds by atomic rearrangement within the domains of the stoichiometric alloy.

This model is supported by the field-ion microscopy of the present study. No domains of ordered structure were observed in the disordered matrix of samples quenched from above the critical temperature. In addition, no "two-phase" structure was observed at any stages of partial order at 700° C. Instead, the ordered regions always impinged, and appeared homogeneous. The order within the domains after short ageing times was imperfect and corresponded closely with that measured by X-ray diffraction techniques. It is interesting to note that the size of the domains in the early stage of ordering, i.e. ~ 40 Å, closely approximates the size of the microdomains calculated by Spruiell [18] for short-range order above T_c.

In the late stages of homogeneous ordering a heterogeneous reaction was initiated at the prior α-grain boundaries. This structure, which appeared to be coherent with one grain and incoherent with the adjacent one (fig. 4), consumed the small domains by the motion of the incoherent interface. The driving force for this process was most likely the decrease in energy of the system obtained by eliminating the antiphase boundaries between the small domains. This heterogeneous component has previously [10, 23] been attributed to a spontaneous recrystallisation process which eliminates the ordering stresses. While this is certainly possible it is felt that the present explanation is more feasible for Ni_4Mo for the following reasons: (a) The process does not occur to any extent at high temperatures [23]; (b) ordering in Ni_4Mo at low temperatures should produce less concentrated stresses than high-temperature ordering since the domains are smaller, and the lattice parameters of the ordered and disordered phases differ to a lesser degree [51]. The low occurrence of the heterogeneous reaction at 775° C can then be attributed to the formation of large nuclei and a low nucleation frequency resulting in a large domain size.

Although the present study did not include "high-temperature" investigations, the ideas presented above on ordering in Ni_4Mo are not inconsistent with the results of other workers at higher temperatures [23].

4.2. Mechanical Behaviour

The remarkable mechanical property changes which accompany ordering reactions have been attributed to a variety of mechanisms [3, 5, 6]. Since many of these mechanisms can operate simultaneously in an alloy, it is very difficult to present a quantitative discussion of their effects. Therefore, only a qualitative correlation between the structure and the mechanical behaviour of Ni_4Mo will be attempted.

Any discussion of the mechanical properties

of ordered alloys must be made in terms of dislocation motion. It has been shown [5, 6] that one significant factor is whether slip dislocations move singularly or in pairs as superdislocations. In view of the small domain structure observed at all stages of ageing in the present study, this factor will be considered first. The diameter of these domains was less than the calculated value of the spacing between paired dislocations of most ordering systems [5]. Similar calculations were made for Ni_4Mo by assuming the glide plane to be the $\{111\}_C$ and the superdislocation to be composed of pairs of unit dislocations of the type $1/2 <110>_C$. The antiphase domain boundary energy for these calculations was determined using a modification of Flinn's [52] method (see appendix). The separation was determined for various degrees of order for the most favourable condition for splitting, i.e. for a pure edge total dislocation. In all cases, except for $S \leqq 0.2$, the separation was less than the corresponding domain size, indicating a high probability for the presence of superdislocations in this system.

The improvement in strength of Ni_4Mo during ordering at 700° C can be attributed to both the domain size and the degree of order. Cottrell [53] has suggested a strengthening mechanism which depends on the creation of a new domain boundary as slip dislocations intersect old boundaries. This mechanism should contribute significantly in the present case since the domains are relatively small. However, since their size is approximately constant after 40 min of ageing this mechanism does not account for the continuous rise in strength. This rise must be explained in terms of the development of the ordered structure within the domains. It cannot, however, be attributed to the destruction of order by dislocation motion since the motion of superdislocations does not destroy order across the glide plane. However, the ordering process in Ni_4Mo produces a tetragonal distortion which should resist dislocation motion. Since the distortion increases as the degree of order increases, this effect qualitatively explains the continuous strength increase during ageing.

The decrease in ductility with ordering at 700° C can be attributed to a number of factors. One factor is a lowering of the probability of dynamic recovery by cross-slip. Another factor is the increased tendency for the formation of co-planar dislocation arrays. This can result from the confinement of dislocations to their slip planes in ordered alloys and the reduction of possible slip systems [54]. Once the co-planar arrays are formed, pile-ups occur at interfaces, such as grain-boundaries, and result in large local stresses across the boundaries. When these stresses are sufficient, intergranular fracture occurs. Another mechanism resulting in brittle intergranular fracture may involve the heterogeneous reaction which occurs along the grain-boundaries. The antiphase domains in these regions are large compared to the fine domain structure of the homogeneous component. These regions should be softer owing to the presence of fewer domain boundaries and the higher probability of superdislocation motion. Slip concentrated in these areas could result in failure along the grain-boundaries where they are formed.

Failure along grain-boundaries during ordering, as was observed in the present study at 750 and 800° C, has been observed in another system [10], and attributed to the ordering stresses. At 750 and 800° C the distortions due to the difference in volume of the ordered and disordered phases in Ni_4Mo, can cause large internal stresses. The resultant direction and magnitude of these stresses is dependent on the frequency of nucleation and the critical nuclei size.

5. Summary

The structural modifications which accompany ordering of Ni_4Mo during isothermal ageing at 700° C have been correlated with the mechanical behaviour of this material. The ordering reaction was found to proceed homogeneously until late in the process when a heterogeneous reaction was initiated along the grain-boundaries. The increase in strength was attributed to the domain size and the stresses induced due to the tetragonality of the ordered phase. The decrease in ductility was attributed to either the development of dislocations in co-planar arrays or concentrated slip in the heterogeneous component.

Acknowledgement

We gratefully acknowledge many helpful discussions with Dr R. W. Newman. In addition, we would like to thank Doctors W. B. Snyder, C. R. Brooks, and E. E. Stansbury for furnishing the results of their work on Ni_4Mo prior to publication, and to Mr R. Mitchell for preparation of the figures. This work was supported by the United States Atomic Energy Commission under

contract no. AT-(40-1)-3908.

Appendix

Calculation of Antiphase Boundary Energy

The antiphase boundary energy was calculated using the procedure outlined by Flinn [52] with certain modifications to account for the structure of Ni_4Mo. The basic equation is:

$$\frac{\text{energy}}{\text{area}} = \left(\frac{\text{atoms}}{\text{area}}\right) \times \left(\frac{\text{wrong bonds}}{\text{atom}}\right) \times \left(\frac{\text{energy}}{\text{wrong bond}}\right). \quad (1)$$

In order to simplify the calculation, the following assumptions were made: (a) Only nearest neighbour interactions are significant. (b) The tetragonal contractions accompanying ordering can be neglected. (c) Since Ni–Ni nearest neighbours are present in the ordered structure and Mo–Mo nearest neighbours are absent, the only wrong bonds that need be considered are Mo–Mo nearest neighbours.

The energy per wrong bond according to the Bragg-Williams approximation [55] for an AB alloy is given by

$$\nu = \frac{kT_c}{2F_A F_B Z}, \quad (2)$$

where T_c is the critical ordering temperature, F_A and F_B are the atomic fractions of the components and Z is the co-ordination number. The parameter ν is defined by the relation:

$$\nu = \nu_{AB} - (\nu_{AA} + \nu_{BB})/2 \quad (3)$$

and is based on the fact that for an AB alloy the interchange of an A and B pair results in the conversion of a certain number of correct A–B bonds in equal numbers of wrong A–A and B–B bonds. The co-ordination number enters the equation by considering the fact that each α-site is surrounded by Z β-sites. In the present case the situation is somewhat different since each Mo-atom is surrounded by twelve Ni-sites and each Ni-site is surrounded on the average by three Mo- and nine Ni-sites. When this factor is considered along with the fact that the composition is 1/5 Mo and 4/5 Ni we obtain a weighted average value for ν according to the equation:

$$\bar{\nu} = 1/5\left(\frac{kT_c}{2(4/5)\,(1/5)\,12}\right) + 4/5\left(\frac{kT_c}{2(4/5)\,(1/5)\,3}\right). \quad (4)$$

Using a value of 1141° K for T_c we obtain

$$\bar{\nu} = \frac{\text{energy}}{\text{wrong bond}} \simeq 14 \times 10^{-14} \text{ ergs.}$$

The number of wrong bonds per atom is determined from the expression

$$\sum_n \vec{t}_n \vec{R}_{hkl} \quad (5)$$

where $\vec{t}$ denotes a wrong bond vector and $\vec{R}$ is the reciprocal lattice vector of the *hkl* plane on which the antiphase boundary lies, i.e. $|\vec{R}_{hkl}| = 1/d_{hkl}$. The sum is evaluated with the restriction that only positive integral values are considered since this is the necessary condition for the bond to cross the plane. In order to determine the possible wrong bond vectors $\vec{t}$, we must first consider the number of unique antiphase translation vectors. Ruedl *et al* [56] have shown that for Ni_4Mo there are only two: $\vec{P}_1 = a_0'/5$ [210] and $\vec{P}_2 = a_0'/5$ [130] both expressed in tetragonal indices. Because of the symmetry of the crystal structure of Ni_4Mo it is sufficient to calculate the antiphase boundary energy for only one of these vectors, say $\vec{P}_1$, and it is convenient to express it in cubic indices; i.e. $\vec{P}_1 = a_0/2$ [110].

A translation of this type generates three Mo–Mo wrong bonds per Mo-atom described by the vectors $\vec{t}_1 = a_0/2$ [110], $\vec{t}_2 = a_0/2$ [0$\bar{1}\bar{1}$], $\vec{t}_3 = a_0/2$ [0$\bar{1}$1], again expressed in cubic indices.

The number of atoms per unit area in an fcc lattice is given by:

$$d_{hkl}/\text{vol. primitive cell} = 4/a_0^2\sqrt{h^2 + k^2 + l^2}. \quad (6)$$

Since in the present case wrong bonds originate only on Mo-atoms, the atomic packing and the stacking sequence of the various *hkl* planes must be considered. Two types of planes are encountered in this structure [21, 57]. There are mixed species planes containing both Mo- and Ni-atoms which give rise only to fundamental reflections and there are single species or layered planes (one layer in five being a Mo layer) which give rise to superlattice as well as fundamental reflections. For the mixed planes a factor of 1/5 must be included in the atoms per area expression given by equation 6 and for the layered planes the value of $\vec{t}_n \cdot \vec{R}_{hkl}$ must be replaced by unity for values less than five, since for this case there cannot be more than one wrong bond per atom.

Following the procedure outlined above the antiphase boundary energy was determined for

various *hkl* planes assuming perfect order. The plane of least energy was found to be $(0\,1\,1)_C$ and that of maximum energy to be $(3\,1\,0)_C$. These values, along with that of the $(1\,1\,1)_C$ are: $E_{011} = 0.28\bar{v}/a_0^2$; $E_{310} = 1.27\bar{v}/a_0^2$; $E_{111} = 0.37\bar{v}/a_0^2$.

Superlattice Dislocation Separation

Ruedl *et al* [56] have shown that a possible superdislocation arrangement in Ni_4Mo consists of a pair of $1/2\ \langle 1\,1\,0\rangle_C$ unit dislocations moving on a $\{1\,1\,1\}_C$ glide plane. If the separation of the unit dislocations into partials is neglected the equilibrium spacing between them is determined by a balance between their mutually repulsive force and the attractive force arising from the antiphase boundary energy. This balance leads to the expression [58]:

$$r = \frac{Gb^2}{2\pi E_{111} S^2}\left[\frac{\cos(\theta + \pi/3)\cos\theta}{1-\nu} + \sin(\theta + \pi/3)\sin\theta\right] \quad (7)$$

where r is the separation distance and θ and $\theta + \pi/3$ represent the angles subtended between the Burgers vector and the dislocation line. The term S^2 must be introduced to account for the fact that the antiphase boundary energy is decreased by this factor when $S < 1$ [59]. The maximum separation occurs when the total Burgers vector of the superdislocation is in an edge orientation, i.e. $\theta = 150°$. Using relation 7 along with a value of $G = 0.75 \times 10^{-5}$ dyne/Å and $\nu = 1/3$ leads to the results below:

TABLE AI

Long-range order parameter, S	Separation in Å
1.0	5
0.8	8
0.6	14
0.4	31
0.2	125

References

1. P. A. FLINN, "Strengthening Mechanisms in Solids" (ASM Seminar, Metal Park, Ohio, 1962).
2. N. F. FIORE and C. L. BAUER, "Progress in Materials Science", edited by Bruce Chalmers, **13**, No. 2 (Pergamon Press, New York, 1967).
3. J. B. COHEN, *J. Mater. Sci.* **4** (1969) 1012.
4. A. KELLY and R. B. NICHOLSON, "Progress in Materials Science", edited by Bruce Chalmers, **10** (Pergamon Press, New York, 1963).
5. N. S. STOLOFF and R. G. DAVIES, *ibid* **13**, No. 1 (Pergamon Press, New York, 1966).
6. R. W. CAHN, "Local Atomic Arrangements Studied by X-ray Diffraction", edited by J. B. Cohen and J. Hilliard (Gordon and Breach, New York, 1967).
7. B. E. WARREN, "X-ray Diffraction" (Addison-Wesley Publishing Company, Reading, Mass., 1969).
8. J. B. COHEN, "Recent Developments Concerning the Order-Disorder Transformation". Paper presented at the 1968 ASM Seminar on Phase-Transformations, Detroit, Michigan, October, 1968.
9. D. HARKER, *J. Chem. Phys.* **12** (1944) 315.
10. V. S. ARUNACHALAM and R. W. CAHN, *J. Mater. Sci.* **2** (1967) 160.
11. V. I. SYUTKINA and E. S. YAKOVLEVA, *Phys. Stat. Sol.* **21** (1967) 465.
12. D. W. PASHLEY, J. L. ROBERTSON, and M. J. STOWELL, *Phil. Mag.* **19** (1969) 83.
13. P. V. GUTHRIE and E. E. STANSBURY, "X-ray and Metallographic Study of the Nickel-Rich Alloys of the Nickel-Molybdenum System II", USAEC Report ORNL-3078, Oak Ridge National Lab., Tennessee, July, 1961.
14. F. H. ELLINGER, *Trans. ASM* **30** (1942) 607.
15. A. N. DUBROVINA and YA. S. UMANSKI, *Russian Metallurgy* **4** (1966) 56.
16. S. J. BLOCH, "Hardness Changes During the Ordering Reaction of Three Nickel-Molybdenum Alloys", M.S. Thesis, Univ. of Tenn. (1960).
17. B. T. LAMPE, "An Investigation of the Order-Disorder Transformation in the Ni-Mo Alloy by Electrical Resistivity Measurements", M.S. Thesis, Univ. of Tenn. (1963).
18. J. E. SPRUIELL and E. E. STANSBURY, *J. Phys. Chem. Sol.* **26** (1965) 811.
19. E. RUEDL, P. DELAVIGNETTE, and S. AMELINCKX, *Phys. Stat. Solidi* **28** (1968) 305.
20. B. G. LEFEVRE, A. G. GUY, and R. W. GOULD, *Trans. Met. Soc. AIME* **242** (1968) 788.
21. B. G. LEFEVRE, H. GRENGA, and B. RALPH, *Phil. Mag.* **18** (1968) 1127.
22. B. G. LEFEVRE and R. W. NEWMAN, Proceedings of Symposium on Field-Ion Microscopy in Physical Metallurgy and Corrosion, Georgia Institute of Technology, Atlanta, Ga., May, 1968.
23. W. B. SNYDER and C. R. BROOKS, "Mechanical Properties and Domain Structure of Ordered Ni_4Mo", presented at the Third Bolton Landing Conference, AIME, September 1969, to be published.
24. E. A. STARKE JR. and E. U. LEE, *Mats. Res. Bull.* **2** (1967) 231.
25. B. G. LEFEVRE and E. A. STARKE JR., "Advances in X-ray Analysis", Vol. 12 (Plenum Press, New York, 1969) p. 113.
26. P. R. SWANN and J. NUTTING, *J. Inst. Met.* **90** (1961) 133.
27. G. THOMAS, *Acta Met.* **11** (1963) 1369.
28. W. BELL, W. R. ROSER, and G. THOMAS, *ibid* **12** (1964) 1247.

29. W. BELL, P. OKAMOTO, and G. THOMAS, *ibid* **13** (1965) 559.
30. Y. CALVAYRAC and M. FAGARD, *Compt. Rend.* **258** (1964) 4531.
31. M. J. MARCINKOWSKI, in "Electron Microscopy and Strength of Crystals" (John Wiley, New York, 1963) p. 333.
32. L. E. TANNER, *Phys. Stat. Solidi* **30** (1968) 685.
33. *Idem*, "The Transformation to Long-Range Order in Ni_2V", presented at the Third Bolton Landing Conference, September, 1969, to be published.
34. *Idem*, *Phil. Mag.* **14** (1966) 111.
35. H. N. SOUTHWORTH and B. RALPH, *ibid* **14** (1966) 383.
36. R. W. NEWMAN and J. J. HREN, *ibid* **16** (1967) 211.
37. T. T. TSONG and E. W. MÜLLER, *J. Appl. Phys.* **38** (1967) 545.
38. *Idem*, *ibid*, 3531.
39. T. T. TSONG, *Surface Sci.* **10** (1968) 303.
40. B. RALPH in "Field-Ion Microscopy", edited by J. J. Hren and S. Ranganathan (Plenum Press, New York, 1968).
41. F. N. RHINES and J. B. NEWKIRK, *Trans. ASM* **45** (1953) 1029.
42. S. C. MOSS and P. C. CLAPP, Technical Report No. 156, Ledgemont Laboratory, Lexington, Mass., November, 1967.
43. G. BORELIUS, *J. Inst. Met.* **74** (1948) 17.
44. G. C. KUCZYNSKI, R. F. HOCHMAN, and M. DOYAMA, *J. Appl. Phys.* **26** (1955) 871.
45. J. L. O'BRIEN and G. C. KUCZYNSKI, *Acta Met.* **7** (1959) 803.
46. J. B. NEWKIRK, A. H. GEISER, D. L. MARTIN, and R. SMOLUCHOWSKI, *Trans. AIME* **188** (1950) 1249.
47. T. T. TSONG and E. W. MÜLLER, *J. Appl. Phys.* **38** (1967) 545.
48. H. N. SOUTHWORTH and B. RALPH, "Conference on Mechanisms of Phase Transformations in Crystalline Solids", Manchester, July, 1968 (Institute of Metals).
49. P. S. RUDMAN, in "Intermetallic Compounds", edited by J. H. Westbrook (John Wiley & Sons, New York, 1967).
50. J. W. CHRISTIAN, "The Theory of Transformations in Metals and Alloys" (Pergamon Press, Oxford, 1965) p. 202.
51. E. E. STANSBURY and J. R. RIDDLE, private communication.
52. P. A. FLINN, *Trans. AIME* **218** (1960) 145.
53. A. H. COTTRELL, "Properties and Microstructure" (ASM, Cleveland, Ohio, 1954).
54. N. S. STOLOFF and R. G. DAVIES, *Acta Met.* **12** (1964) 473.
55. W. L. BRAGG and E. J. WILLIAMS, *Proc. Roy. Soc.* **A145** (1934) 699; **A151** (1935) 54; E. J. WILLIAMS, *ibid* **A152** (1935) 231.
56. E. RUEDL, P. DELAVIGNETTE, and S. AMELINCKX, *Phys. Stat. Solidi* **28** (1968) 788.
57. B. G. LEFEVRE, E. A. STARKE JR., and S. SPOONER, *Surf. Sci.* **14** (1969) 266.
58. J. FRIEDEL, "Dislocations" (Addison-Wesley Publishing Co., Reading, Mass., 1964).
59. M. J. MARCINKOWSKI and D. S. MILLER, *Phil. Mag.* **6** (1961) 871.

Received 6 January and accepted 12 February 1970.